J|A|C|S ARTICLES

Published on Web 02/06/2009

In Situ Observation of Rapid Ligand Exchange in Colloidal Nanocrystal Suspensions Using Transfer NOE Nuclear Magnetic Resonance Spectroscopy

Bernd Fritzinger,[†] Iwan Moreels,[‡] Petra Lommens,[‡] Rolf Koole,[§] Zeger Hens,[‡] and José C. Martins*,[†]

NMR and Structure Analysis Unit, Ghent University, Krijgslaan 281-S4, B-9000 Ghent, Belgium, Physics and Chemistry of Nanostructures, Ghent University, Krijgslaan 281-S12, B-9000 Ghent, Belgium, and Condensed Matter and Interfaces, Faculty of Science, Utrecht University, Princetonplein 1, NL-3508 TH Utrecht, The Netherlands

Received December 3, 2008; E-mail: Jose.Martins@UGent.be

Abstract: Recently, solution NMR-based approaches have been developed that represent useful new tools for the in situ characterization of the capping ligand in colloidal nanocrystal dispersions. So far, this development has focused mainly on tightly bound ligands (no exchange) or ligands in slow exchange with the nanocrystal surface. In such systems, the ligand can be identified and its amount and interaction quantified via 1D ^{1}H NMR, ^{1}H−^{13}C HSQC, and DOSY spectra. Here, we explore the case where capping ligands are in fast exchange with the nanocrystal surface. Using dodecylamine-stabilized CdTe (Q-CdTe|DDA) and octylamine-stabilized ZnO (Q-ZnO|OctA) nanoparticles, we first show that the NMR methods developed so far fail to evidence the bound ligand when the effect of the latter on the exchange-averaged parameters is marginalized by an excess of free ligand. Next, transfer NOE spectroscopy, a well-established technique in biomolecular NMR, is introduced to demonstrate and characterize the interaction of a ligand with the nanocrystal surface. Using Q-PbSe nanocrystals capped with oleic acids as a reference system, we show that bound and free ligands have strongly different NOE spectra wherein only bound ligands develop strong and negative NOEs. For the Q-CdTe|DDA system, transfer NOE spectra show a similar rapid appearance of strong, negative NOEs, thereby unambiguously demonstrating that DDA molecules spend time at the nanocrystal surface. In the case of Q-ZnO|OctA, where a more complex mixture is analyzed, transfer NOE spectroscopy allows distinguishing capping from noncapping molecules, thereby demonstrating the screening potential offered by this technique for colloidal quantum dot dispersions.

1. Introduction

The synthesis of nanocrystals using a bottom-up approach based on colloid chemistry has gained considerable popularity over the past two decades. The so-called hot injection method yields stable dispersions of colloidal nanocrystals with diameters in the 1−15 nm range.[1,2] These particles consist of an inorganic core surrounded by a shell of organic capping molecules or ligands. Clearly, the nature, size, and shape of the inorganic core are of primary importance, for it is the core that determines the (quantum) properties of the nanocrystals.[3−5] However, the role of the organic ligands is not negligible and has been receiving increasingly more attention.[6] Typical ligands consist of a functional headgroup that binds to the nanocrystal surface and an organic tail that is exposed to the environment. Since the head groups adsorb at the nanocrystal surface, they play a crucial role in synthesis, where they help to control the size and shape of the particles.[6] The tail, possibly with a functional end group, determines the interaction of the nanocrystals with their surroundings in terms of solubility in particular solvents and affinity for specific surfaces or chemicals.[7,8] This makes capping engineering—that is, making nanocrystals in which the ligands display a variety of desirable properties—an important topic in colloidal nanocrystal research, especially in view of the increasing demand for tailor-made nanocrystals for the study of biological systems and the formation of complex, nanocrystal-based superstructures. Progress in this respect is inextricably linked to a better understanding of the surface−ligand and ligand−ligand interactions at the nanocrystal−ligand interface.

[†] NMR and Structure Analysis Unit, Ghent University.
[‡] Physics and Chemistry of Nanostructures, Ghent University.
[§] Condensed Matter and Interfaces, Utrecht University.

(1) Murray, C. B.; Norris, D. J.; Bawendi, M. G. *J. Am. Chem. Soc.* **1993**, *115*, 8706.
(2) Murray, C. B.; Sun, S. H.; Gaschler, W.; Doyle, H.; Betley, T. A.; Kagan, C. R. *IBM J. Res. Dev.* **2001**, *45*, 47.
(3) Klimov, V. I.; Ivanov, S. A.; Nanda, J.; Achermann, M.; Bezel, I.; McGuire, J. A.; Piryatinski, A. *Nature* **2007**, *447*, 441.
(4) Moreels, I.; Lambert, K.; De Muynck, D.; Vanhaecke, F.; Poelman, D.; Martins, J. C.; Allan, G.; Hens, Z. *Chem. Mater.* **2007**, *19*, 6101.
(5) Yu, H.; Li, J. B.; Loomis, R. A.; Wang, L. W.; Buhro, W. E. *Nat. Mater.* **2003**, *2*, 517.
(6) Yin, Y.; Alivisatos, A. P. *Nature* **2005**, *437*, 664.
(7) Hyun, B. R.; Chen, H. Y.; Rey, D. A.; Wise, F. W.; Batt, C. A. *J. Phys. Chem. B* **2007**, *111*, 5726.
(8) Hens, Z.; Tallapin, D. V.; Weller, H.; Vanmaekelbergh, D. *Appl. Phys. Lett.* **2002**, *81*, 4245.

 10.1021/ja809436y CCC: $40.75

Recently, we[9−12] and others[13−20] have demonstrated the potential of solution-state NMR spectroscopy for the investigation of colloidal nanocrystal ligands. While sensitivity can be an issue, NMR provides distinct advantages over other techniques. First, suspensions can be studied in situ with minimal perturbation. Second, each molecular species can be monitored individually and therefore give information on its chemical environment, provided the species contribute resolved signals. In most NMR studies reported so far, bound ligand resonances that appear markedly different from those of the free ligands were observed. This indicates that the exchange of the ligand between the free and the bound states, if any, proceeds at a rate that is slow with respect to the frequency time scale, with an upper limit typically in the s^{-1} range (*no or slow* exchange). This situation is well suited to ligand identification, especially when combined with pulsed field gradient diffusion NMR techniques that allow differentiation of the various species according to their translational diffusion coefficients.[9−11] Using diffusion ordered spectroscopy (DOSY), the resonances of the free and surface-bound ligands can be separated along the diffusion dimension since the ligand exchange rate proved to be slow on the diffusion time scale as well in these cases. In addition to identification of free and bound species, application of ^{1}H NMR enables quantification of the ligand density at the nanocrystal surface. Furthermore, semiquantitative information as to the surface−ligand adhesion and ligand−ligand interaction energies can also be obtained, as previously demonstrated for InP with trioctylphosphine oxide ligands. In summary, a well-established set of techniques and methods has become available to study ligand capping in the case of *no or slow* ligand exchange.

Here we discuss the application of solution NMR analysis to nanocrystal dispersions where the kinetics of ligand exchange between the free and the bound states is fast on the time scales of interest. Using dodecylamine-stabilized CdTe (Q-CdTe|DDA) and octylamine-stabilized ZnO (Q-ZnO|OctA) nanoparticles, we find that such fast exchange compromises the extraction of relevant information regarding the capping ligand. Instead of individual characteristics of the free and the bound states, population-averaged chemical shifts and diffusion coefficients are obtained. However, we show that, under these circumstances, ligands that interact with the nanocrystal surface can be conclusively identified via transfer NOE (trNOE) spectroscopy.[21−23] This technique is well known in the field of biomolecular NMR, where it has found widespread application in screening for and conformational analysis of small-molecule ligands bound to macromolecular targets such as receptor proteins and enzymes.[21−26] trNOE exploits the presence of a fast exchange process and couples it to the difference in sign and buildup rate of intraligand ^{1}H−^{1}H NOEs imparted by the different molecular tumbling rates for the ligand in the bound and free states. Binding of the ligand to a protein is unambiguously demonstrated when strong, negative NOEs, which can only be acquired by the ligand in the protein-bound state, are visible between or "transferred to" the exchange-averaged ligand resonances. Given that certain conditions are satisfied, the conformation of the ligand when bound to the protein receptor can also be determined. We show that this technique can also be applied to the case of a capping ligand interacting with a nanocrystal surface under fast exchange conditions.

To investigate whether the bound ligand state satisfies the prerequisite for the development of strong and negative NOEs required for trNOE spectroscopy, we first studied a model system consisting of PbSe nanoparticles capped with tightly bound oleic acid ligands (Q-PbSe|OA).[11] Here, only the bound ligand contributes to the ^{1}H spectrum of a Q-PbSe|OA dispersion, and the rapid development of strong, negative NOEs is indeed observed in 2D NOESY spectra. Since capping ligands, such as OA, have very weak NOEs when free in solution, one might expect therefore that the strong, negative NOEs built up by a ligand while bound to the nanocrystal surface will outweigh those of the free state and dominate the NOESY spectrum, even when the free state is present to a considerable excess.[21−23] This is exactly what is observed with Q-CdTe|DDA and Q-ZnO|OctA. This makes it possible to establish the presence and identity of ligands in fast exchange with the nanocrystal surface, and it creates the possibility to screen ligands for their relative binding potential. The trNOE approach thus complements the solution NMR techniques already developed for colloidal dispersions where the kinetics of capping ligand exchange falls in the slow exchange regime, and opens up the possibility to develop screening techniques allowing the detection of binding ligands in complex solute/solvent mixtures.

2. Theoretical Basis

2.1. Fast Exchange in 1D and DOSY ^{1}H NMR. In NMR, chemical exchange refers to a situation where nuclear spins are exchanged between different environments or sites where they have different NMR observables, P_s.[27−29] These include the chemical shift, relaxation rate, and diffusion coefficient. Typically, conformational processes or association phenomena are responsible for driving the exchange process. In the situation of interest here, a free ligand, L, binds to a free site on a nanocrystal surface, NC•, thereby becoming a bound ligand, L-NC. This is most simply written as

(9) Hens, Z.; Moreels, I.; Martins, J. C. *ChemPhysChem* **2005**, *6*, 2578.
(10) Moreels, I.; Martins, J. C.; Hens, Z. *ChemPhysChem* **2006**, *7*, 1028.
(11) Moreels, I.; Fritzinger, B.; Martins, J.; Hens, Z. *J. Am. Chem. Soc.* **2008**, *130*, 15081.
(12) Van Lokeren, L.; Maheut, G.; Ribot, F.; Escax, V.; Verbruggen, I.; Sanchez, C.; Martins, J. C.; Biesemans, M.; Willem, R. *Chem.−Eur. J.* **2007**, *13*, 6957.
(13) Aldana, J.; Wang, Y. A.; Peng, X. G. *J. Am. Chem. Soc.* **2001**, *123*, 8844.
(14) Majetich, S. A.; Carter, A. C.; Belot, J.; Mccullough, R. D. *J. Phys. Chem.* **1994**, *98*, 13705.
(15) Sachleben, J. R.; Colvin, V.; Emsley, L.; Wooten, E. W.; Alivisatos, A. P. *J. Phys. Chem. B* **1998**, *102*, 10117.
(16) Ribot, F.; Escax, V.; Roiland, C.; Sanchez, C.; Martins, J. C.; Biesemans, M.; Verbruggen, I.; Willem, R. *Chem. Commun. (Cambridge, U. K.)* **2005**, 1019.
(17) Liu, H. T.; Owen, J. S.; Alivisatos, A. P. *J. Am. Chem. Soc.* **2007**, *129*, 305.
(18) Steckel, J. S.; Yen, B. K. H.; Oertel, D. C.; Bawendi, M. G. *J. Am. Chem. Soc.* **2006**, *128*, 13032.
(19) Kohlmann, O.; Steinmetz, W. E.; Mao, X. A.; Wuelfing, W. P.; Templeton, A. C.; Murray, R. W.; Johnson, C. S. *J. Phys. Chem. B* **2001**, *105*, 8801.
(20) Shen, L.; Soong, R.; Wang, M. F.; Lee, A.; Wu, C.; Scholes, G. D.; Macdonald, P. M.; Winnik, M. A. *J. Phys. Chem. B* **2008**, *112*, 1626.
(21) Clore, G. M.; Gronenborn, A. M. *J. Magn. Reson.* **1982**, *48*, 402.
(22) Ni, F. *Prog. Nucl. Magn. Reson. Spectrosc.* **1994**, *26*, 517.
(23) Meyer, B.; Weimar, T.; Peters, T. *Eur. J. Biochem.* **1997**, *246*, 705.
(24) Meyer, B.; Peters, T. *Angew. Chem., Int. Ed.* **2003**, *42*, 864.
(25) Jimenez-Barbero, J.; Asensio, J. L.; Canada, F. J.; Poveda, A. *Curr. Opin. Struct. Biol.* **1999**, *9*, 549.
(26) Peters, T.; Pinto, B. M. A. *Curr. Opin. Struct. Biol.* **1996**, *6*, 710.
(27) Sandström, J. *Dynamic NMR Spectroscopy*; Academic Press: London/New York, 1982.
(28) Gutowsky, H. S.; Holm, C. H. *J. Chem. Phys.* **1956**, *25*, 1228.
(29) Bain, A. D. *Prog. Nucl. Magn. Reson. Spectrosc.* **2003**, *43*, 63.

$$L + NC^{\bullet} \rightarrow L\text{-}NC \quad (1)$$

From the perspective of a ^{1}H nucleus in the ligand, this represents a two-site (free/bound) second-order exchange, a situation that has been well described for the case of protein−ligand interactions. In terms of kinetics, the adsorption rate, r_{on}, is of second order in the concentrations of L and NC$^{\bullet}$, with rate constant k_{on}, while the desorption rate, r_{off}, is of first order in the concentration of the bound ligands, with rate constant k_{off}. The lifetime constant of a ligand ^{1}H nucleus in the free (τ_L) and bound states ($\tau_{L\text{-}NC}$) is then given by

$$\tau_L = 1/(k_{on}[NC^{\bullet}]) \quad (2)$$

$$\tau_{L\text{-}NC} = 1/k_{off} \quad (3)$$

To discuss the effects of chemical exchange on spectral properties, it is convenient to characterize the process by a single lifetime, τ_{ex}, and associated exchange rate k_{ex}, defined as

$$k_{ex} = 1/\tau_{ex} = 1/\tau_{L\text{-}NC} + 1/\tau_L = k_{off} + k_{on}[NC^{\bullet}] = k_{off}(1 + x_{L\text{-}NC}/x_L) \quad (4)$$

where x_L and $x_{L\text{-}NC}$ correspond to the molar fractions of the free and bound ligands in solution. When free ligand is present in large excess ($x_{L\text{-}NC} \ll x_L$), k_{ex} tends to k_{off}. The presence of slow, intermediate, or fast exchange conditions is dependent on the value of k_{ex} with respect to the difference, ΔP, in the NMR property of interest, as follows:

$$k_{ex} \ll \Delta P \quad \text{slow exchange} \quad (5)$$

$$k_{ex} \approx \Delta P \quad \text{intermediate exchange} \quad (6)$$

$$k_{ex} \gg \Delta P \quad \text{fast exchange} \quad (7)$$

When P refers to the frequency or a relaxation rate (both longitudinal R_1 and transversal R_2), the frequency and relaxation time scales are defined respectively as

$$\Delta P_\nu = |\nu_{free} - \nu_{bound}|; \quad \Delta P_R = |R_{1,2,free} - R_{1,2,bound}| \quad (8)$$

For the case of diffusion NMR spectroscopy, the diffusion time scale is defined by the inverse of the diffusion delay Δ, such that ΔP should be equal to Δ^{-1} in the equations above.

For the Q-PbSe|OA and other similar cases studied before, slow exchange conditions apply and the free and bound species and their associated NMR properties, P_L and $P_{L\text{-}NC}$, can be observed separately. When fast exchange conditions apply, as will be the case for the Q-CdTe|DDA and Q-ZnO|OctA, the NMR property P will adopt an average value, P_{obs}, determined by its respective value in the free and the bound states scaled by their respective fractional populations (x_L and $x_{L\text{-}NC}$, respectively):

$$P_{obs} = x_L P_L + x_{L\text{-}NC} P_{L\text{-}NC} = P_L + (P_{L\text{-}NC} - P_L) x_{L\text{-}NC} \quad (9)$$

The intermediate case is not of interest here and will not be further discussed. More in-depth treatment of chemical exchange is available in the literature.[27,29]

2.2. NOE and Transfer NOE. The nuclear Overhauser effect (NOE) between dipolar coupled ^{1}H nuclei is best known from its application in structural and conformational analysis of molecules. This results from the fact that its intensity is determined in part by the internuclear ^{1}H−^{1}H distance according to an r^{-6} dependency. It can be measured using a variety of techniques. Here, such effects are most conveniently obtained using 2D NOE spectroscopy (NOESY), where cross-peaks occur at the frequency coordinates of the interacting ^{1}H spin pair with a volume that reflects the NOE's intensity.[30,31] The interesting property from our point of view, however, is that the sign and buildup rate of the NOE are dependent on the rotational correlation time, τ_c, of the molecule in which the ^{1}H pair is embedded. For a rigid spherical particle with radius r and solvent viscosity η, τ_c is determined by the well-known Stokes−Einstein relation:

$$\tau_c = \frac{4\pi\eta r^3}{3k_B T} \quad (10)$$

When τ_c is much smaller than the reciprocal of the spectrometer's angular frequency ω_0^{-1} (the so-called extreme narrowing limit), a molecule will develop positive NOEs at a slow rate (typically $\sigma \approx 0.1$ s^{-1}) (small-molecule behavior). On the other hand, a molecule with a τ_c much larger than ω_0^{-1} (the so-called spin-diffusion limit) is characterized by a more rapid development (typically $\sigma \approx 10$ s^{-1}) of large negative NOEs (large-molecule behavior). This change in sign is linked to the contribution to the overall NOE buildup rate of two opposing cross-relaxation pathways with different sensitivity to the molecular reorientational motion. When going from fast to slow tumbling, the two opposing pathways will balance each other out at some point, and a zero cross-over occurs around $\tau_c \approx \omega_0^{-1}$, i.e., the inverse of the spectrometer ^{1}H frequency. Working at a ^{1}H spectrometer frequency of 500 MHz, the associated zero cross-over τ_c is ∼0.3 ns. With a viscosity of 0.556 mPa·s (toluene), we calculate $\tau_c = 15$ ns for a particle with a radius of 3 nm at 298 K, and only $\tau_c = 70$ ps for one of 0.5 nm radius. Therefore, we can expect that free ligand molecules will generally behave like small molecules and develop weak, positive or even no NOEs due to a small positive or zero cross-relaxation rate constant, σ_L. On the other hand, a ligand bound to a macromolecular object such as a nanocrystal should rapidly develop large and negative NOEs due to a large but negative cross-relaxation rate constant, $\sigma_{L\text{-}NC}$. From a practical viewpoint, it is important to realize that a positive (negative) NOE will lead to a cross-peak with opposite (same) sign with respect to the diagonal peaks in the 2D NOESY spectrum.[21]

Transfer NOE spectroscopy exploits this difference in cross-relaxation rates by coupling it to a situation where the ligand is in fast exchange on the relaxation time scale. As discussed in more detail elsewhere,[22] the averaged cross-relaxation rate, $\langle\sigma\rangle$, responsible for the buildup of the NOE intensity is then given by

$$\langle\sigma\rangle = x_L\sigma_L + x_{L\text{-}NC}\sigma_{L\text{-}NC} \quad (11)$$

and will be dominated by the bound state, at least as long as the inequality

$$|x_{L\text{-}NC}\sigma_{L\text{-}NC}| \gg |x_L\sigma_L| \quad (12)$$

is satisfied. Given that σ_L is generally much smaller than $\sigma_{L\text{-}NC}$, this inequality is easily satisfied under fast exchange conditions, even when $x_{L\text{-}NC} \ll x_L$, i.e., in the presence of an excess of free ligand. In other words, the large, negative NOE developed by the ligand while present at the binding site will easily outweigh the small, positive NOE acquired while free in solution, even when the ligand is present in considerable excess. At the same time, these conditions yield a single, exchange-averaged set of resonances with line width and position near those of the free ligand due to the latter's excess. All combined, therefore, large, negative trNOEs will appear in the 2D NOESY spectrum between ^{1}H ligand resonances with characteristics of the free

(30) Jeener, J.; Meier, B. H.; Bachmann, P.; Ernst, R. R. *J. Chem. Phys.* **1979**, *71*, 4546.
(31) Macura, S.; Huang, Y.; Suter, D.; Ernst, R. R. *J. Magn. Reson.* **1981**, *43*, 259.

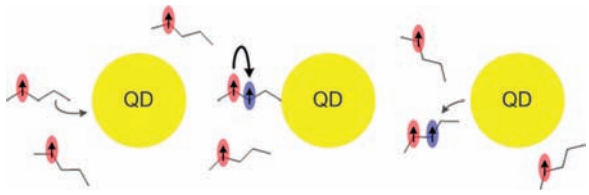

Figure 1. The trNOE concept: upon adsorption at the quantum dot surface, the tumbling rate of the ligand slows down and an initial polarization located at specific protons can be efficiently distributed via the NOE effect to neighboring protons during the mixing time. This distributed polarization is maintained after desorption, when the ligand's tumbling rate increases again, and appears as a cross-peak in the 2D NOESY spectrum. NOEs generated in the bound state are thus effectively transferred to the free state. Additionaly, as the latter is present in excess, these *transfer* NOEs will appear at frequencies dominated by the free ligand. Molecules that did not interact with the surface develop no or very weak NOEs and therefore do not contribute to the NOESY spectrum.

ligand (Figure 1) at fairly short mixing times, typically 50−100 ms.[21] Inversely, the presence of such trNOEs between ligand resonances in the presence of a macromolecular object unambiguously establishes that it is involved in a fast exchange process between a bound state and a free state. Thus, the presence and identity of a binding ligand are easily established, even in the presence of a mixture containing other non-interacting ligands.

3. Experimental Section

PbSe nanocrystals featuring oleic acid ligands (Q-PbSe|OA) were prepared by hot injection of a mixture of $Pb(OA)_2$ and trioctylphosphine selenium (TOP-Se) in diphenyl ether, following the synthesis published by Murray et al.[2] DDA-stabilized Q-CdTe nanoparticles were prepared by slowly heating a mixture of dimethylcadmium (ARC Technologies, 99.9%), elementary tellurium (Heraeus, 99.999%), TOP (Fluka, >90%), and DDA (Aldrich, 98%) according to the procedure published by Wuister et al.[32] Q-ZnO stabilized by OctA (Acros Organics, 99+%) was prepared starting from the synthesis reported by Schwartz et al.,[33] followed by a ligand exchange as described in ref 34.

Q-PbSe|OA and Q-CdTe|DDA NMR samples were prepared in deuterated toluene (99 atom % D). To prevent aging and degradation of Q-PbSe|OA by oxidation, the dispersion was transferred into a screw-cap NMR tube (Wilmad LabGlass, Buena, NJ) inside a glovebox flushed with N_2. Q-ZnO|OctA did not dissolve in pure toluene, and a mix of deuterated toluene and chloroform was used instead. Apart from the solvents, the Q-ZnO sample also contains residues of ethanol and DMSO that were used during synthesis and purification. For comparison purposes, solutions of pure OA, DDA, and OctA were prepared in solvent formulations identical to those used for all three nanocrystal systems. All experiments were performed on a Bruker Avance DRX 500 spectrometer, operating at a ^{1}H and ^{13}C frequency of 500.13 and 125.76 MHz, respectively, and equipped with a 5 mm TXI probe with Z-gradient affording a maximum gradient strength of 0.5350 T m^{-1}. The temperature was set to 298 K for Q-PbSe|OA and Q-CdTe|DDA and to 288 K for Q-ZnO|OctA. All 1D and 2D spectra were recorded using standard pulse sequences from the Bruker pulse program library in TopSpin 1.3. All processing was performed using TopSpin 2.1 unless mentioned otherwise. All spectra were referenced using the residual ^{1}H signal of the toluene solvent as a secondary reference against TMS. The 1D ^{1}H spectra were recorded with a spectral width of 10.00 ppm (5000 Hz), 16−32 scans, and a 10 s relaxation delay (d1) to allow full relaxation between scans. The FID was sampled using 32 768 points for an acquisition time of 3.2768 s. ^{1}H−^{13}C heteronuclear single quantum coherence (HSQC) specta were recorded using adiabatic 180° inversion pulses, GARP decoupling, and gradient selection of the desired coherence pathway. Typically 256 t_1 increments, consisting of four scans of 2048 sampled data points each, were recorded with a 1.5 s relaxation delay and a ^{1}H and ^{13}C spectral width of 10.00 and 120.00 ppm, respectively. 2D NOESY spectra were recorded using a ^{1}H spectral width of 10.00 ppm. Typically 256 t_1 increments, consisting of 16 scans of 2048 sampled data points each, were recorded with a 2 s relaxation delay. Processing consisted of apodization with a squared cosine window function, followed by zero-filling before Fourier transformation to a 2048 × 2048 complex data set. NOE mixing times used varied from 1 to 1000 ms. A polynomial baseline correction was applied when appropriate. To determine the NOE buildup, 2D NOESY with mixing times of 1, 5, 10, 15, 20, 25, 50, 75, 100, 150, 200, 300, 500, and 1000 ms were recorded. The peak volumes were determined via integration of rectangular peak areas using TopSpin 2.1. Diffusion experiments were performed with the approach described previously.[10] The diffusion parameters, consisting of the gradient pulse length δ and the diffusion delay Δ, were chosen such that a signal decay of roughly 90% was obtained at the highest gradient strength used. The gradient strength was varied from 2 to 98% of the maximum strength using a smoothed squared gradient shape. A slightly modified version of the monopolar convection-compensated sequence was used throughout.[35] All DOSY processing was performed using the GIFA-DOSYm software package, applying an inverse Laplace transform regularized with a maximum entropy algorithm. Diffusion coefficients were extracted by analyzing the original signal decays using the Steijskal Tanner equation in the matNMR package for Matlab.[36] Values were found to be identical within experimental error to those extracted directly from the DOSY data.

4. Results

4.1. Initial Characterization of the Q-CdTe|DDA Dispersion. Figure 2 shows the 1D and 2D ^{1}H−^{13}C HSQC spectra of a suspension of 3.9 nm DDA-stabilized Q-CdTe in toluene, together with reference measurements on a solution of DDA in toluene. One sees that the presence of Q-CdTe does not lead to additional resonances, while the ^{1}H and ^{13}C chemical shifts are at best minimally perturbed by the presence of Q-CdTe. The ^{1}H chemical shift of the well-resolved α-CH_2 (2.55 ppm) and methyl (0.97 ppm) resonances of Q-CdTe|DDA differ by only 2 and 3 Hz, respectively, from those observed in the blank DDA solution. This contrasts with previous studies on InP, TiO_2, CdSe, and PbSe, where a distinct set of resonances can immediately be recognized for the bound and free ligand in solution.[9−12] Here, however, no resonances typically associated with capping ligands in such a slow exchange situation could be detected. Shifting the focus to translational diffusion measurements using DOSY, we find that all DDA resonances in the Q-CdTe|DDA suspension show a single exponential decay as a function of field gradient strength, which results in a single DOSY peak with an average diffusion coefficient of 1.35 × 10^{-9} m^2/s (Figure 3a). This is a reduction by only 6% compared to that for DDA in the blank solution (D = 1.45 × 10^{-9} m^2/s) and much larger than the value of 1 × 10^{-10} m^2/s typically expected for a particle with a 3.9 nm diameter in toluene. Importantly, we also noted that the value of the diffusion

(32) Wuister, S. F.; van Driel, F.; Meijerink, A. *Phys. Chem. Chem. Phys.* **2003**, *5*, 1253.
(33) Schwartz, D. A.; Norberg, N. S.; Nguyen, Q. P.; Parker, J. M.; Gamelin, D. R. *J. Am. Chem. Soc.* **2003**, *125*, 13205.
(34) Lommens, P.; Loncke, F.; Smet, P. F.; Callens, F.; Poelman, D.; Vrielinck, H.; Hens, Z. *Chem. Mater.* **2007**, *19*, 5576.
(35) Jerschow, A.; Müller, N. *J. Magn. Reson.* **1997**, *125*, 372.
(36) van Beek, J. D. *J. Magn. Reson.* **2007**, *187*, 19.

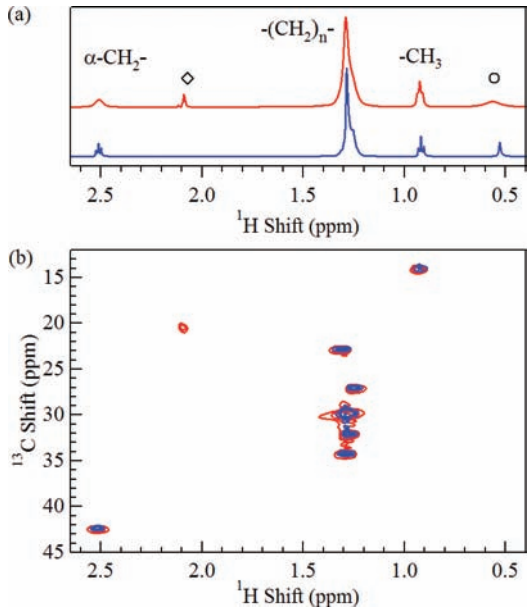

Figure 2. Comparison of 1D ^{1}H spectra (a) and 2D ^{1}H−^{13}C HSQC spectra (b) in toluene-d_8 of pure DDA (blue) and Q-CdTe|DDA (red). For the latter, a preparation for which maximal line width effects are observed in the ^{1}H NMR spectrum was selected. ○ indicates a pool of exchangeable protons contributed by the amine function and traces of residual water; ◇ marks the residual toluene solvent signal, which is observed only in the more dilute Q-CdTe|DDA sample.

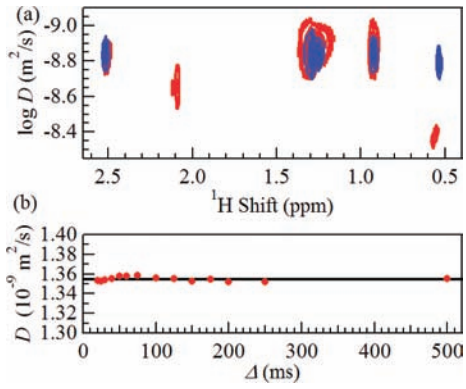

Figure 3. (a) Comparison of 2D DOSY spectra in toluene-d_8 of pure DDA (blue) and Q-CdTe|DDA (red), indicating quasi identical diffusion coefficients for DDA. The signals at 0.55 ppm arise from a pool of exchangeable protons contributed by the amine function and traces of residual water. At 2.11 ppm, the residual toluene solvent signal is visible; it is observed only in the more dilute Q-CdTe|DDA sample. (b) Extracted diffusion coefficient plotted as a function of diffusion time Δ, indicating the absence of any dependence on this parameter.

coefficient does not depend on the diffusion delay Δ, even when the latter is reduced to 20 ms (Figure 3b).

Depending on the exchange regime, a number of possible explanations exist for these observations. In the case of *no or slow* exchange between bound and free DDA ($k_{ex} < \Delta P$), the absence of a second species in the frequency and diffusion dimensions could result from a strong line-broadening of the bound ligand resonances and/or from the presence of too small a fraction of bound species.[37] Either of these conditions would make it difficult to observe an NMR signal for the bound DDA ligand, and the measured observables will correspond to free

(37) Millet, O.; Loria, J. P.; Kroenke, C. D.; Pons, M.; Palmer, A. G. *J. Am. Chem. Soc.* **2000**, *122*, 2867.

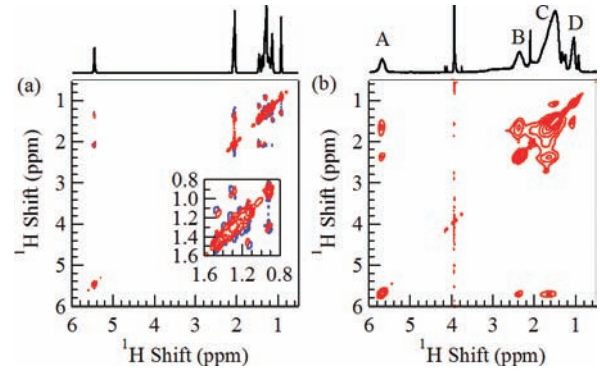

Figure 4. NOESY spectra of OA in toluene (a) and of Q-PbSe with OA (b) recorded with 100 ms mixing time. In presence of Q-PbSe, strong, negative NOE cross-peaks involving all OA signals are visible. The reference sample of OA in toluene, on the other hand, shows only zero-quantum coherence cross-peaks, typically recognized from their antiphase line shape, as evident from the inset. Thus, no NOE cross-peak intensity has evolved within the given mixing time, clearing the path for trNOE measurements.

DDA. However, since previously studied systems with *no or slow* exchange (PbSe, InP, TiO_2, CdSe) always showed bound ligand resonances,[9−20] the presence of slow exchange for the Q-CdTe|DDA case appears rather unlikely. In view of the small but notable perturbations of the spectrum, a rapid exchange ($k_{ex} > \Delta P$) of the DDA between the solution and the Q-CdTe surface appears more plausible. Assuming fast exchange conditions, eq 2 shows that the observed NMR property will be averaged over those of the free and bound states. Since we find that the chemical shifts, and especially line widths and diffusion coefficients, of the DDA ligand are almost equal to those of free DDA, we must assume that $x_L \gg x_{L\text{-}NC}$. In principle, evidence establishing a fast exchange regime can be obtained via the dependence of the perturbation $P_{obs} - P_L$ on the bound fraction $x_{L\text{-}NC}$, with $P_{L\text{-}NC} - P_L$ fixed. Unfortunately, our observations show that we are already in a situation where $P_{obs} \cong P_L$, and thus $x_L \gg x_{L\text{-}NC}$. Since it proved difficult to obtain stable suspensions with a reduced amount of DDA ligand, this dependency could not be exploited. Therefore, the evidence for stabilization of CdTe by DDA and fast exchange between bound and free DDA is only circumstantial at this point. However, the presumed fast exchange conditions should allow direct demonstration of ligand binding in a 2D NOESY spectrum via the trNOE phenomenon.

4.2. Bound Ligands Have Strong, Negative NOEs. The evolution of trNOEs via 2D NOESY critically depends on the ability of the capping ligand to rapidly generate strong, negative NOEs while bound to the nanocrystal surface (see Theoretical Basis). Therefore, we first present results of 2D NOESY measurements on Q-PbSe|OA, which is a system with tightly bound ligands that show no measurable exchange.[11] Here, the bound oleic acid ligands can be monitored independently, allowing the NOE characteristics of the bound state to be established without interference from the exchange process. The 1D spectrum of PbSe|OA features four prominent resonances related to OA: the alkene protons at 5.69 ppm; the methylene protons next to the alkene protons at 2.36 ppm; a broad, unresolved methylene resonance at 1.49 ppm; and the methyl resonance at 1.04 ppm (ref 11 and top of Figure 4b).

In Figure 4, we show the 100 ms 2D NOESY spectrum of a Q-PbSe|OA dispersion and that of a blank OA solution in toluene. The various cross-peaks visible in the blank solution,

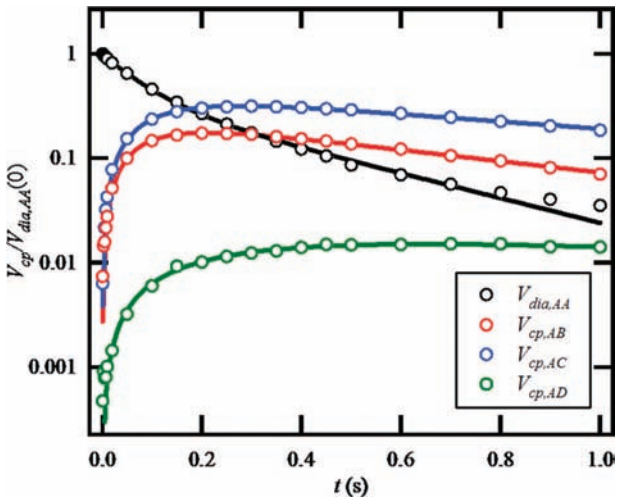

Figure 5. Buildup of the three detectable NOE cross-peaks involving the alkene protons in PbSe|OA and the decay of the diagonal alkene proton resonance. All intensities are given relative to the initial intensity of the diagonal alkene proton peak. The corresponding peaks can be located via the labels in Figure 4b.

e.g., between the isochronous alkene ^{1}H and the vicinal CH_2 units, show antiphase fine structure that is typical for zero-quantum coherence artifacts between scalar coupled spins. No NOE cross-peaks are apparent at this relatively short mixing time, as can be expected for this small molecule. In contrast, the Q-PbSe|OA dispersion shows strong, negative NOE cross-peaks between all resolved resonances at 100 ms mixing time. More specifically, prominent NOEs from the alkene protons toward the neighboring methylenes and to the unresolved methylene groups in the chain are apparent. A weak NOE can even be seen to the end chain methyl group. NOESY spectra with similar appearance have been reported for gold nanoclusters capped with thiopronin.[19] We conclude that the rotational mobility of a bound capping ligand molecule is dominated by the overall rotational diffusion behavior of the nanocrystal, which leads to the development of a strong, negative NOE.

To investigate this in more detail, the NOE cross-peak intensity buildup was monitored as a function of the NOE mixing time in the range from 1 to 1000 ms. Figure 5 shows the time evolution of the NOE cross-peaks that involve the well-resolved alkene protons at 5.69 ppm. Especially for these NOEs, the buildup and the decay of the NOE cross-peak signal intensity volume, $V_{cross}(t)$, can be described fairly well using a simple model:

$$\frac{V_{cross}(t)}{V_{dia}(0)} = A\, e^{-R_L t}(1 - e^{-R_C t}) + B \qquad (13)$$

Here, R_L is the overall T_1 longitudinal relaxation rate describing the return to equilibrium, and R_C is the cross-relaxation rate giving rise to the NOE transfer, while $V_{dia}(0)$ denotes the initial intensity of the diagonal peak associated with the alkene proton resonance. When appropriate, a constant B is added to correct for minor integration artifacts. The prefactor A is the relative volume the NOE cross-peak would attain if no longitudinal relaxation occurred. As such, it yields the fraction of the spin polarization that is transferred from the diagonal peak to the cross-peak. As summarized in Table 1, we find an NOE transfer rate of 11 ± 1 s^{-1} and a prefactor A of 0.25. The rate is in excellent agreement with values typical for large proteins. The prefactor value shows that 25% of the initial spin polarization of the alkene protons is transferred by cross-relaxation to the neighboring methylene protons. For transfer to the end-chain methyl group, the rate decreases to 3.7 ± 1 s^{-1} and the prefactor is reduced to only 3.7% of $V_{dia}(0)$. Summed over all detectable cross-peaks, the prefactors amount to 73% of $V_{dia}(0)$. Since the NOEs involving OA resonances close to the carboxylic acid moiety and nanocrystal surface are not observable due to excessive line broadening, this value indicates that essentially every OA molecule in the system develops negative NOEs, as could be expected here since only bound ligands are present. It should be noted that the longitudinal relaxation rate R_L determined here agrees well with previously published values.[11]

4.3. Transfer NOEs in DDA Support Fast Exchange in Q-CdTe|DDA. The 100 ms 2D NOESY spectrum of the Q-CdTe|DDA dispersion is shown in Figure 5, together with that of a DDA blank solution. As for oleic acid, no NOE cross-peaks are apparent between the DDA resonances at 100 ms in the blank solution. Only zero-quantum coherence artifacts that are developed between scalar coupled resonances during the NOE mixing time can be seen. When the NOE mixing time is extended to 600 ms, these artifacts diminish due to multiple quantum relaxation during the mixing time and weak positive NOEs (oppositely signed to the diagonal peaks) appear. Interestingly, a weak, positive cross-peak is also found that connects the αCH_2 to the pool of labile hydrogens. As the latter represents labile hydrogens in fast exchange between the DDA amine function and traces of water, this can be understood as a combination of an NOE between the α-methylene and the amine function and exchange with water.

The 2D NOESY spectrum of the Q-CdTe|DDA dispersion has a markedly different appearance (Figure 6b). A strong cross-peak indicative of a negative NOE is clearly apparent between the αCH_2 and the methylene chain resonance at 100 ms mixing time. A clear negative NOE also links this methylene chain to the end methyl group. In addition, a weak, negative NOE also develops between the αCH_2 and the end methyl group. From these observations, the presence of a fast exchange transfer process is conclusively established since the negative NOEs can only be generated while the DDA ligand is bound to the Q-CdTe surface. The observed NOEs must therefore be considered trNOEs. The pool of labile hydrogen, which is considerably broadened here, also features cross-peaks with all DDA resonances. This suggests a combination of the NOEs involving the ligand resonances with an exchange process involving the amine and residual water in the sample.

Looking at the buildup curves, we find a picture that is comparable to that of PbSe|OA. Figure 7 shows the intensity buildup of the cross-peaks that involve the αCH_2 at 2.55 ppm, relative to the initial intensity $V_{dia}(0)$, of the diagonal αCH_2 resonance. The curves were fitted to eq 13, and the resulting fitting parameters have been summarized in Table 1. Taking the cross-peak to the methylene chain resonances at 1.33 ppm, we find a buildup rate of 7.7 ± 0.5 s^{-1} and a prefactor that amounts to 66% of $V_{dia}(0)$. For the NOE cross-peak between the αCH_2 resonance and the end methyl, the buildup rate is reduced to 2 ± 0.2 s^{-1}, and the prefactor equals 6%. Finally, the NOE cross-peak with the pool of labile protons builds up at a rate of 11.0 s^{-1}, with a prefactor amounting to 25% of $V_{dia}(0)$. Summed over all resonances, the prefactors correspond to 97% of the original intensity of the αCH_2 resonance. Similar to the observation for PbSe|OA, this brings us to the conclusion that every DDA molecule in the system acquires negative NOE cross-peaks.

Table 1. Fitting Parameters Obtained for a Set of NOE Cross-Peak Buildup Curves Measured at PbSe|OA and Q-CdTe|DDA

system	PbSe|OA[a]			CdTe|DDA[b]		
cross-peak	AB (5.72/2.39)	AC (5.72/1.65)	AD (5.72/1.09)	AB (2.55/1.33)	AC (2.55/0.97)	AD (2.55/0.66)
A	0.24	0.45	0.037	0.66	0.063	0.25
R_L (s^{-1})	1.28	0.83	0.76	0.39	<0.2	1.33
R_C (s^{-1})	10.8	8.7	1.9	7.8	2.12	10.9
B				−0.017	−0.0020	

[a] All cross-peaks involve the alkene proton resonance at 5.72 ppm. [b] All cross-peaks involve the αCH_2 at 2.55 ppm.

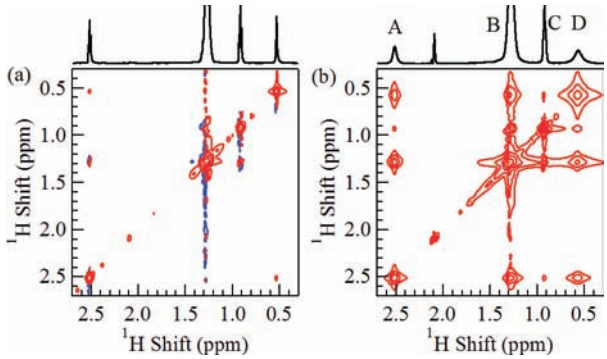

Figure 6. 2D NOESY spectra at 100 ms mixing time of a reference DDA sample in toluene (a) and of Q-CdTe with DDA (b). Whereas zero-quantum coherence artifacts typical for small molecules are visible in the reference sample, strong, negative trNOE cross-peaks are apparent in Q-CdTe|DDA. The peak AD, linking the αCH2 and the labile hydrogen pool, at 0.55 ppm represents the combined NOE and exchange transfer between them via the amine function.

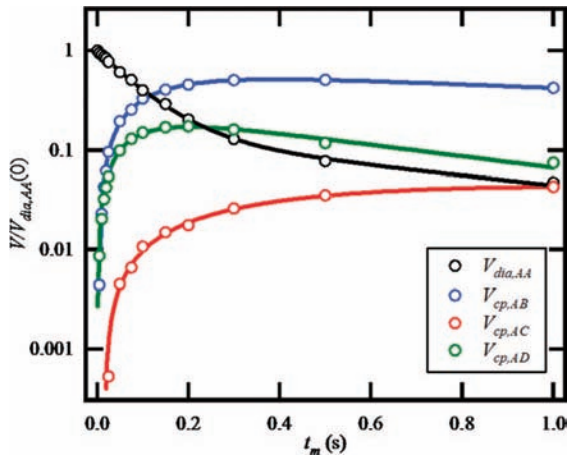

Figure 7. Buildup of the three detectable NOE cross-peaks involving the αCH_2 in CdTe|DDA and the decay of the diagonal αCH_2 resonance. All intensities are given relative to the initial intensity of the diagonal αCH_2 resonance. The corresponding peaks can be located via the labels in Figure 6b.

5. Discussion

5.1. Fast Exchange in CdTe|DDA. On the basis of 1D ^{1}H, 2D ^{1}H−^{13}C HSQC, and DOSY, we find that the suspension of DDA in CdTe colloidal quantum dots shows only minimal changes of chemical shifts, a slight line broadening, and a small decrease of the diffusion coefficients. Such results are anomalous for a tightly bound ligand, and we interpreted them in terms of fast chemical exchange under conditions of a free ligand excess. This hypothesis is substantiated by the 2D NOESY experiment that clearly displays trNOE cross-peaks. In contrast to free DDA, we observe a buildup of negative trNOE cross-peaks between different DDA protons in a Q-CdTe|DDA suspension. Moreover, on the basis of the overall intensity of the cross-peaks with the αCH_2—where the prefactors sum up to 97% of the initial intensity—we conclude that every DDA molecule essentially spends time at the CdTe surface in the course of the NOESY measurement.

Having demonstrated the presence of fast exchange, we can use the initial characterization of the Q-CdTe|DDA system for a more quantitative analysis of the exchange process. Combining eq 9 with the experimental data, an upper limit for $x_{L\text{-}NC}$ can be found. In previously studied nanocrystal dispersions with the capping ligand in slow exchange, the chemical shift difference $\Delta\delta = \delta_{L\text{-}NC} - \delta_L$ typically ranged from 0.1 to 0.3 ppm, i.e., 50−150 Hz at 500 MHz. The 2−3 Hz perturbation of the chemical shift observed in the Q-CdTe|DDA dispersion here allows $x_{L\text{-}NC}$ to be estimated to be 2−6%. A similar value of about 5% is obtained when the DDA diffusion coefficients D_L and $D_{L\text{-}NC}$ are used instead of the chemical shifts. In addition, a lower limit for the desorption rate constant, k_{off}, can be obtained from the DOSY measurements, where the same average diffusion coefficient is obtained from $\Delta = 1$s down to $\Delta = 20$ ms. This means that $k_{ex} \approx k_{off} \gg 50\ s^{-1}$.

5.2. Interpretation of Transfer NOEs from Quantum Dot Ligands. Can any relevant information be extracted from the trNOE intensity buildup in fast exchanging systems (Q-CdTe|DDA), or from the NOE buildup in slow exchanging ones (e.g., Q-PbSe|OA) for that matter? From theoretical treatments of the trNOE in protein−ligand complexes, it should be clear that the fraction of bound ligand is only one of many parameters influencing the trNOE response.[22,38] Provided certain conditions are met, intraligand distances between protons may be extracted and used to derive the conformation of the bound ligand. Unfortunately, this cannot be extrapolated to the capping ligand on colloidal quantum dots, as that situation is fundamentally different from the protein−ligand case. For proteins, the number of ligand binding sites is generally limited, a 1:1 stoichiometry being observed in many cases. In addition to the contribution of intramolecular NOEs, proton spins from the surrounding protein may also contribute to the NOE transfer pathways between ligand protons, and these effects need to be taken into account, for instance, by a full exchange−relaxation matrix analysis based on the known structure of the binding site.[22,38,39] For the case of Q-NC, a high number of binding sites are available to the ligands, and depending on the surface coverage, each ligand may be in contact with multiple neighboring ligand chains. In this case, therefore, both intra- and interchain cross-relaxation pathways will occur and contribute to the observed NOE cross-peak intensity. Also, depending on the local inter-proton correlation times along the chain, efficient spin diffusion may occur, leading to multispin contributions. Given the undoubtedly larger variability in the surface composition and

(38) Ni, F. *J. Magn. Reson. B* **1995**, *106*, 147.
(39) Moseley, H. N. B.; Curto, E. V.; Krishna, N. R. *J. Magn. Reson. B* **1995**, *108*, 243.

structure of the individual ligand binding sites, a simple universal model cannot be formulated. As a result, an interpretation of the trNOE intensity or buildup in terms of the conformational properties of the capping ligand should, in our opinion, not be attempted. A possible approach to learn more about the cross-relaxation contributions could be the use of fully deuterated capping ligands doped by a small amount, e.g. <5%, of protonated ones. As these are not readily available for the ligands used here, this was not further investigated.

For the same reasons outlined above, interpretation of the individual NOEs in terms of ligand conformations should be done with great care. In the case of Q-PbSe|OA, for instance, the end-chain methyl group is seen to generate a weak-intensity NOE cross-peak with the alkene moiety. This NOE could be explained as a direct NOE contact. Indeed, the high surface coverage in Q-PbSe|OA, determined to be about 4 molecules·nm^{-2},[11] and the presence of a kink in the chain, caused by the cis C9−C10 alkene conformation, may allow a fraction of the OA methyls to come in direct proximity of the alkene ^{1}H's in neighboring OA chains.[11] However, the presence of a similar trNOE in the Q-CdTe|DDA case, involving the end-chain methyl and the αCH_2, suggests spin diffusion along the chain as a more likely origin of this trNOE cross-peak. Therefore, we interpret the cross-relaxation rate constants obtained from the NOE (no exchange) and trNOE (exchange) buildup curves as effective rate constants that represent the net effect of a more complicated transfer process comprising intra- and intermolecular NOE transfer by direct NOE contacts and/or spin diffusion.

6. Validation and Application of trNOE Spectroscopy

From the above, it appears that trNOE spectroscopy is a valid tool to establish fast chemical exchange kinetics in situations where this is only indirectly apparent from the chemical shift and diffusion NMR data. To further evaluate its potential, we focus on a system consisting of Q-ZnO stabilized with octylamine (OctA) in a 90:10 mixture of toluene-d_8 and chloroform-d. This system has a more complicated spectrum than in Q-CdTe|DDA due to the presence of residues of DMSO and ethanol from the synthesis procedure that cannot be easily removed without disturbing the stability of the system. For the NMR analysis, the contribution of the latter two components was reduced by using the deuterated analogues during washing, and a blank sample that tries to closely mimic this mixture was prepared.

From a comparison of the 1D spectra in Figure 8a, only a single set of signals is obtained for OctA. In this case, a broadening and a larger shift of 30 Hz are apparent for the αCH_2 as compared to the Q-CdTe|DDA case. Looking at the HSQC, the βCH_2 also shifts 25 Hz along the ^{1}H dimension, whereas the end methyl is not perturbed. The attribution of these shifts to the contribution of a bound OctA species in fast exchange should be placed in doubt, however, as both the DMSO and the ethanol signals shift as well. This shift may be due to differences in the mixture's composition between the dispersion and the blank, or it could indicate interaction of these species with the Q-ZnO surface. In any case, it places considerable doubts on the use of chemical shift perturbations to indicate interaction with the nanocrystal surface.

The diffusion coefficient measured for OctA in the blank sample was 1.37×10^{-9} m^2/s, whereas in the Q-ZnO dispersion, a value of 1.19×10^{-9} m^2/s is obtained—that is, a 13% reduction

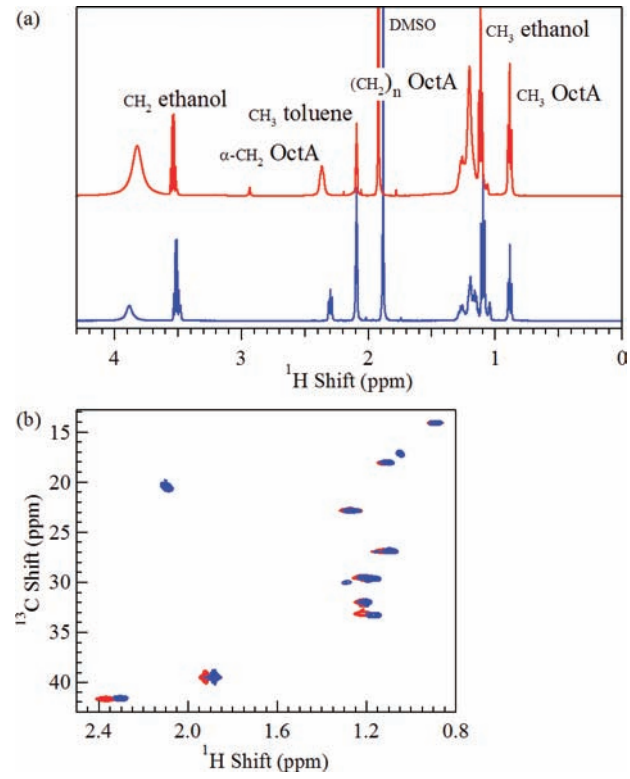

Figure 8. (a) 1D proton spectra in toluene-d_8 (top) of OctA in a Q-ZnO dispersion (red) and in a blank solution (blue) with approximately the same mixture of other small-molecule components, as indicated. (b) Detail of the ^{1}H−^{13}C HSQC of both samples, shown superimposed, highlighting the small differences in the OctA chemical shift in the presence of Q-ZnO.

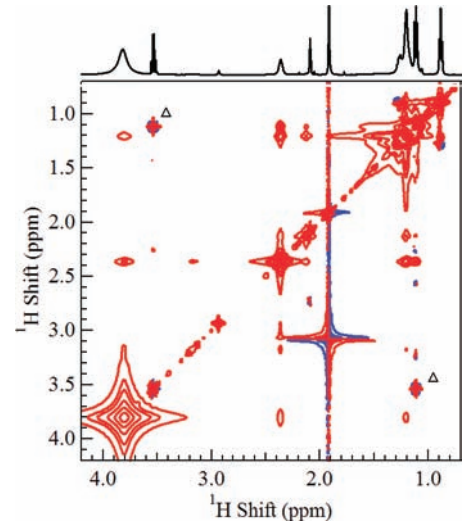

Figure 9. NOESY spectra with 100 ms mixing time of Q-ZnO|OCTA, illustrating strong, negative NOEs involving the OctA resonances, while zero-quantum coherence cross-peaks are clearly apparent for ethanol (Δ).

in diffusion coefficient. Nevertheless, this value is again too large for a particle with a nanocrystal core diameter of about 4 nm.

To evaluate the presence of fast exchange, 100 ms NOESY spectra were measured (Figure 9). For the blank sample, only zero-quantum coherence cross-peaks were visible for any of the species. In the presence of Q-ZnO, however, strong, negative trNOEs are apparent between the OctA resonances, but not between ethanol resonances. This shows that, of all species

present, only OctA spends time on the surface of Q-ZnO, albeit in rapid exchange with a pool of free OctA. The lack of intermolecular trNOEs to the DMSO and ethanol resonances also suggests that the latter do not come into contact with the capping layer.

This example shows the usefulness of trNOE as a tool to screen for capping ligands with fast exchange kinetics. Even in complicated solvent mixtures, a relative affinity ranking can be established, much in the same way as described for protein−ligand interactions. Also, impurities may be present in the starting materials used for nanocrystal synthesis or for ligand exchange. When these would be present at sufficient concentrations to be detectable via NMR, and provided they show distinct signals, their ability to interact with the nanocrystal surface under fast exchange conditions should also be recognizable from the occurrence of negative trNOE cross-peaks in the 2D NOESY spectra, depending on the relative affinity and concentration. Obviously, when the impurity is too low in concentration to be detectable by NMR, its presence will escape notice. It can be expected, however, that under these conditions it should not be a major contributor to surface capping.

7. Conclusions

We could demonstrate that nanocrystal−ligand systems in fast exchange can be studied with solution NMR by combining an elementary characterization based on 1D proton NMR, $^{1}H-^{13}C$ HSQC, and DOSY NMR data with transfer NOE spectroscopy. For the Q-CdTe|DDA system, the elementary characterization gives results that are all close to the characteristics of free DDA, which means that there is no direct evidence for stabilization of Q-CdTe by DDA. Using Q-PbSe|OA, where the ligands are tightly bound to the nanocrystal (no exchange), we demonstrate that bound and free ligands have strongly different NOE spectra, where only bound ligands rapidly develop strong and negative NOEs. Despite being dominated by the free DDA, the NOESY experiments on the Q-CdTe|DDA system show a similar rapid appearance of strong, negative NOEs that can be generated only while the DDA ligand is bound to the nanocrystal surface. Consequently, the fact that the DDA chemical shifts and the diffusion coefficient in the Q-CdTe|DDA system are close to the free DDA values is interpreted in terms of fast exchange in the presence of a large excess of free ligands. Thus, the resulting transferred NOEs between the DDA protons build up while the ligand is bound to the nanocrystal surface and are measured after its release. This is a successful application of trNOE, which is well established in biological NMR, to the field of nanocrystal ligand characterization.

To show the practical applicability of the approach, we also applied the same techniques to the Q-ZnO|OctA system. Here, the shifts of the OctA αCH_2 and βCH_2 peaks in the 1D proton and the HSQC experiment in the presence of Q-ZnO already give an indication of fast exchange. This is further supported by the DOSY results, which show a slowing of diffusion in the presence of Q-ZnO. Using again the trNOE technique, we could conclusively demonstrate that OctA acts as fast exchanging ligand, whereas the other molecules in the solution do not interact with the nanocrystal or the capping ligand layer. With this approach, it should even be possible to screen more complex mixtures for possible ligand candidates, under the condition of non-overlapping signals. When considerable ligand excess is required for dispersion stability, such that the usual NMR parameters are dominated by the free ligand's properties, only the trNOE technique allows conclusive assignment of binding ligands.

We conclude that solution-state NMR is a very powerful tool to characterize colloidal nanocrystal dispersions stabilized by organic ligands. After it was shown that NMR is useful to qualitatively and quantitatively characterize systems in no or slow exchange,[9−12] we have now extended its reach to systems with fast ligand exchange. Following our approach, it is possible to decide what molecules in a colloidal dispersion of nanocrystals or other systems—e.g., organic pigment crystals—are in contact with the surface and to analyze their adsorption/desorption behavior: nonexchanging ligands can be distinguished from exchanging ligands and nonligands. This is even possible in complex mixtures resulting from a multistep sample preparation.

Acknowledgment. J.C.M. and Z.H. acknowledge the Fund for Scientific Research−Flanders (FWO-Vlaanderen) and Belgian Science Policy (BelSPo) for various research and equipment grants (J.C.M., G.0365.03 and G.0064.07; Z.H., G.0.144.08 and IAP 6/10 photonics@be). The authors thank Prof. G. A. Morris (Department of Chemistry, Manchester University) for useful discussions and help in optimizing the phase cycle of the monopolar convection compensated pulse sequence. I.M. acknowledges the Institute for the Promotion of Innovation through Science and Technology in Flanders (IWT-Vlaanderen) for a scholarship.

JA809436Y